Marine Chemistry 151 (2013) 47–55

Contents lists available at SciVerse ScienceDirect

Marine Chemistry

journal homepage: www.elsevier.com/locate/marchem

100-year ecosystem history elucidated from inner shelf sediments off the Pearl River estuary, China

Guodong Jia [a,*], Shendong Xu [a], Weifang Chen [b], Fei Lei [a], Yang Bai [a], Chih-An Huh [b]

[a] CAS Key Laboratory of Marginal Sea Geology, Guangzhou Institute of Geochemistry, Chinese Academy of Sciences, Guangzhou 510640, China
[b] Institute of Earth Sciences, Academia Sinica, Taipei, Taiwan

ARTICLE INFO

Article history:
Received 4 August 2012
Received in revised form 13 February 2013
Accepted 14 February 2013
Available online 28 February 2013

Keywords:
Carbon burial
Community structure
Eutrophication
Inner shelf
Sediment record

ABSTRACT

In this paper, we analyze the organic geochemistry of four sediment cores recovered from a cross-shelf transect offshore from the Pearl River Estuary, China, in an attempt to determine the impact of anthropogenic activity on carbon burial and phytoplankton community structure over the past century. Downcore total organic carbon (TOC) was found to be predominantly of marine origin, as indicated by the TOC:TN ratio, $\delta^{13}C_{org}$, and the branched and isoprenoid tetraether (BIT) index. Profiles of degradation-corrected marine organic carbon (MOC_{corr}) show an asynchronous history, with a gradual increase beginning in the 1940s at the proximal sites (A9 and A7), in the 1970s at the central site (A6), and after 2000 at the distal site (A5). Following this gradual increase, a concurrent but more rapid rise in MOC_{corr} occurred after about 1980, except at site A5. This rise in MOC_{corr} is probably associated with enhanced primary productivity related to an increase in the fluvial nutrient influx, as indicated by upcore increases in $\delta^{13}C_{org}$, $\delta^{15}N$, and phyto-sterol lipids. At sites A7 and A6, phyto-sterol compound ratios suggest a progressive decrease in diatoms, but an increase in non-diatom algae in the community since the 1940s. However, inshore at site A9, the community structure, as well as $\delta^{15}N$, remained almost unchanged. Distance from the shore may be one cause of the asynchronous increase in MOC_{corr} along the cross-shelf transect. However, our results imply that changes in community structure may also modulate MOC burial by partially offsetting the effect of growth in primary productivity. In addition, the $CaCO_3$:MOC_{corr} ratio decreased significantly at sites A7 and A6 over the past 30 years, which may suggest a relative decrease in marine carbonate production that may have acted as a negative feedback to limit atmospheric CO_2 rises.

1. Introduction

Coastal seas and estuaries are sites of significant land–sea interaction, and compared with their surface area, these transitional regions along the continental margins play a disproportionately important role in biogeochemical cycles. This is because they not only receive large inputs of carbon and nutrients from the land that stimulates intense biological activity (Smith and Hollibaugh, 1993; Gattuso et al., 1998), but they also exchange large amounts of matter and energy with the open oceans (e.g., Thomas et al., 2004). In addition, during the last century, anthropogenic activities such as fossil fuel combustion, intensive inorganic fertilizer application, land reclamation, deforestation, and the discharge of industrial and municipal waste waters, have resulted in the increased delivery of inorganic nutrients and organic carbon into estuaries and coastal waters (van Beusekom and de Jonge, 2002; Smith et al., 2003) and led to their eutrophication (Cloern, 2001). The resultant environmental consequences (e.g., increased phytoplankton production, oxygen deficiency, and decreased biodiversity) are of major concern because of the well-documented deterioration in the quality of many coastal waters and alterations to the marine food web and community structure (e.g., Cloern, 2001; Diaz and Rosenberg, 2008). The excess of nutrients may locally enhance primary production and carbon sequestration, but can also strongly influence carbon metabolism via a change in the balance between autotrophic and heterotrophic conditions in estuaries and coastal waters (Kemp et al., 1997; Gypens et al., 2009), and hence their ability to pump atmospheric CO_2 (Andersson and Mackenzie, 2004; Mackenzie et al., 2004; Gypens et al., 2009).

The Pearl River is a subtropical river that runs through southern China before discharging into the South China Sea (SCS). It is the second largest river in China in terms of discharge, with an annual average discharge of $>10^4$ m^3 s^{-1}, 80% of which occurs during the wet season (April–September). Like many estuarine ecosystems worldwide, anthropogenic activity has had an increasing impact on the Pearl River Estuary (PRE) because the Pearl River Delta region, with a population of 45.5 million, has become one of the fastest developing regions in China over recent decades. Large volumes of nutrients and carbon are delivered into the PRE, causing eutrophication (Huang et al., 2003), and affecting carbon dynamics (Cai et al., 2004; Dai et al.,

* Corresponding author. Fax: +86 20 85290278.
E-mail address: jiagd@gig.ac.cn (G. Jia).

0304-4203/$ – see front matter © 2013 Elsevier B.V. All rights reserved.
http://dx.doi.org/10.1016/j.marchem.2013.02.005

2008b). Previous research revealed a high partial pressure of CO_2 (pCO_2), of up to 7000 μatm, and hypoxia in the lower section of the river and the upper PRE (Zhai et al., 2005; Dai et al., 2006; Chen et al., 2008; Guo et al., 2008), which is believed to be driven by aerobic respiration and nitrification (Zhai et al., 2005; Dai et al., 2006, 2008a). In contrast, a clear drawdown of pCO_2 in the lower PRE and adjacent coastal waters, reaching a level below or near the atmospheric pCO_2, was observed (Chen et al., 2008; Dai et al., 2008b). This spatial pCO_2 distribution was mirrored by the variability of phytoplankton activity, with low biomass and productivity due to high dilution levels and light limitation (due to the high turbidity) in the freshwater dominated estuary, high biomass and productivity at intermediate salinities in the estuarine/coastal plume, and reduced biomass and productivity due to nutrient limitation in the seawater dominated region (Yin et al., 2004).

While the nutrients, pollutants, carbon system, and ecosystem of the modern PRE and adjacent coastal waters were being investigated, parallel efforts were made to explore its historical context. This focused on the recovery and analysis of short sediment cores that revealed an overall increase in the fluxes of terrestrial material, anthropogenic pollutants, and marine organic matter over the past few decades (e.g., Jia and Peng, 2003; Ip et al., 2004; Owen and Lee, 2004; Liu et al., 2005; Hu et al., 2008, 2009). These changes were attributed to increasing agricultural activity, sewage discharge, marine fish farming, rapid population growth, and industrial development in the Pearl River Delta region, and enhanced soil erosion and delivery of associated nutrients to the PRE.

Most previous studies of the sedimentary record have been limited to areas within the PRE and adjacent waters. These investigations have been critical to developing an understanding of the history of human impacts on the environment of the PRE and adjacent areas, but they have not explored the record preserved in the shelf sediments outside the PRE. In fact, the Pearl River plume extends offshore to cover a large area of the northern SCS during the wet season (Yin et al., 2001; Su, 2004; Liu et al., 2012), and Dai et al. (2008b) recently described a phytoplankton bloom stimulated by this large freshwater plume. By analyzing a 29-year time series of multidisciplinary observational data obtained between 1976 and 2004, Ning et al. (2009) showed that nutrient levels and primary productivity had increased progressively in the northern SCS. However, longer-term biogeochemical changes in this region have not been well documented. Developing a better understanding of temporal and spatial changes to the biogeochemistry of the shelf area in response to human activities in the Pearl River watershed is important, because its drainage basin is located entirely within a heavily populated subtropical zone that is developing rapidly. This area provides an excellent opportunity to study the biogeochemical interaction between large rivers and low-latitude continental shelves.

This study examines the organic and inorganic carbon, and total nitrogen contents, as well as their isotopes and sterol lipid biomarkers, preserved within four sediment cores recovered from a cross-shelf transect off the PRE in the northern SCS. These data allowed us to reconstruct the temporal and spatial changes to the shelf ecosystem driven by human activity.

2. Materials and methods

2.1. Study area

The PRE is a bell-shaped estuary, about 70 km long and with an area of approximately 2000 km^2 (Fig. 1). The width of the PRE varies from about 15 km at its upper end to 35 km at the lower end. Its average water depth is about 4.8 m, but can exceed 20 m in the eastern section of the lower PRE. The freshwater discharge from the Pearl River completes its transition from a river plume to the coastal front around the middle reach of the PRE due to the wide and shallow

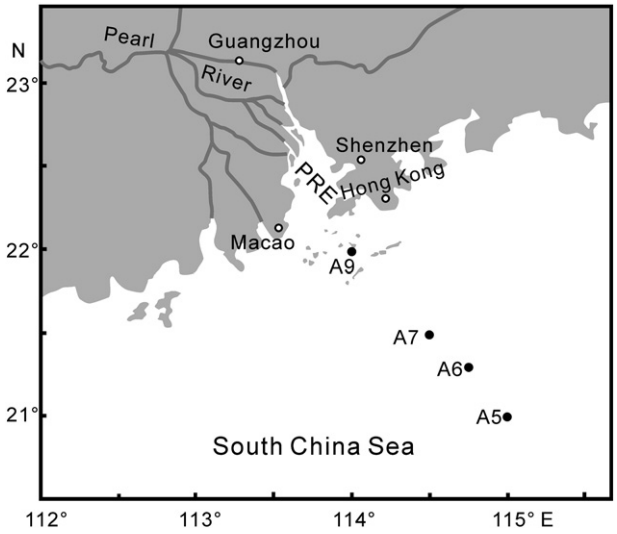

Fig. 1. The study area and sediment core locations (A5–A7 and A9). PRE: Pearl River Estuary.

nature of the estuary there and the relatively small tidal range (Dong et al., 2004; Su, 2004). After exiting the mouth of the estuary, the PRE plume over the shelf has distinct monsoonal characteristics; i.e., it turns toward the west during the dry season, as expected from the gravitational adjustment requirement, but turns to the east during the wet season due to the southwesterly monsoon, when the Pearl River discharge reaches its maximum. The pattern of the offshore river plume during the wet season is rather variable, and may sometimes extend much further to the east beyond the inner shelf, probably due to the many factors influencing its spreading, such as runoff, winds, and coastal currents (Su, 2004; Liu et al., 2012).

The Pearl River has high nutrient concentrations (silicate 130–140 mM, nitrate 75–100 mM, and phosphate 0.2–1.2 mM), and it is thought to be nitrogen unlimited, but phosphorus limited, in the PRE and coastal plume (Yin et al., 2000, 2001; Yin and Harrison, 2008; Cai et al., 2004). The export of the excess N offshore into the oligotrophic water may result in an increase in marine algal blooms (Dai et al., 2008b).

2.2. Sediment cores and sample collection

Box cores A5, A6, A7, and A9 were collected during the China Ocean Carbon (CHOICE-C) Cruise I onboard the *Dongfanghong II* in August 2009. The coring sites were located along a cross-shelf transect southeast of the PRE and Hong Kong, on the inner shelf of the northern SCS (Fig. 1). Core A9 was located inshore and close to the PRE mouth, while cores A5–A7 were located progressively offshore (Table 1).

The core surfaces were well preserved upon collection, as demonstrated by the fairly clear water above the sediment in the box corers. After the overlying water had been siphoned out, core barrels (internal diameter: 11.4 cm, length: 60 cm) were pushed into each box to remove subcores. Sediment in the subcores was then (usually within an hour) extruded onboard using a hydraulic jack, and sectioned at 2-centimeter intervals. The sectioned samples were sealed in plastic jars (internal diameter: 8.5 cm, height: 7.5 cm) and then frozen until they were freeze-dried in the laboratory.

2.3. Analytical methods

2.3.1. Bulk analysis

Sediment total organic carbon (TOC), total nitrogen (TN), and stable isotopic values ($\delta^{13}C_{org}$ and $\delta^{15}N$) were analyzed in duplicate, using an elemental analyzer (Vario Pyro Cube) connected to a continuous flow

Table 1
Information of sediment cores and dating results.

	A5	A6	A7	A9
Core location				
Latitude (N)	21.0	21.3	21.5	22.0
Longtitude (E)	115.0	114.7	114.5	114.0
Water depth (m)	102	89	73	33
Core length (cm)	24	34	20	52
Dating model (CIC)				
Linear accumulation rate (cm $year^{-1}$)	0.21	0.39	0.18	0.61
Mass accumulation rate (g cm^{-2} $year^{-1}$)	0.28	0.33	0.16	0.48
Time span (year)	1901–2006	1902–2008	1906–2006	1926–2008
Mean temporal resolution per 2-cm interval (year)	9.6	6.6	11.1	3.3

system (Isoprime 100), after removal of carbonate with HCl. The average standard deviations of these measurements were ±0.2% for TOC and TN, and ±0.2‰ for $\delta^{13}C_{org}$ and $\delta^{15}N$. Values of $\delta^{13}C_{org}$ and $\delta^{15}N$ are expressed in standard delta notation relative to the Pee Dee Belemnite and atmospheric N_2 standards, respectively. Weight percentages of total carbon (TC) were determined in duplicate (without acidification) by combustion (at 1000 °C) on the Vario Pyro Cube CHN elemental analyzer, and total inorganic carbon (TIC) was determined by difference: TIC = TC − TOC. The $CaCO_3$ content, as the weight percent, was calculated from the TIC content by multiplying the TIC by 8.33, and assuming that all TIC is present as $CaCO_3$.

As shown below, TOC was predominantly of marine origin. Therefore, measured values for $\delta^{13}C_{org}$ are associated with the historic isotope of dissolved inorganic C from which organic C was produced photosynthetically. By assuming that the water mass in our study area was close to a state of equilibrium with the atmospheric ^{13}C Suess effect (caused by the historical increase in ^{13}C-depleted fossil fuel burning), a correction factor was calculated based on an equation modified from Schelske and Hodell (1995):

$$\delta^{13}C = -4.5778 + 7.3430 \times (t-10) - 3.9213 \times 10^{-3} \times (t-10)^2 + 6.9812 \times 10^{-7} \times (t-10)^3 - (-6.31) \quad (1)$$

where t is time (years), and −6.31‰ is the $\delta^{13}C_{atm\text{-}CO_2}$ value in 1840. Here, we use the term (t − 10), instead of t as applied to lake systems by Schelske and Hodell (1995), because a period of 10–12 years is required to establish ^{13}C equilibrium between the ocean and atmosphere (Broecker and Peng, 1974; Lynch-Stieglitz et al., 1995). The calculated time-dependent depletion in $\delta^{13}C$ since 1840 was subtracted from the measured $\delta^{13}C_{org}$ for each dated sediment section.

2.3.2. Lipid biomarker analysis

Each freeze-dried and homogenized sample (ca. 5 g) was successively extracted ultrasonically six times, with MeOH (2×), dichloromethane (DCM)/MeOH (1:1, v/v) (2×), and DCM (2×), and all extracts were then combined after centrifugation. Following saponification and extraction into hexane, the neutral lipids were purified using silica gel chromatography by elution with *n*-hexane and DCM/MeOH (1:1, v/v), respectively. Sterols and glycerol dialkyl glycerol tetraethers (GDGTs), the target compounds in this study, were separated with the DCM/MeOH fraction. The solvent of this fraction was removed under N_2, and the residue was dissolved by sonication (for 5 min) in hexane/propanol (99:1, v/v), and then divided into two parts. One part was used to quantify the sterol compounds after derivatization (as trimethylsilyl ether derivatives) by gas chromatography (GC; Hewlett Packard 6890 with FID) by comparison of their peak areas to that of methyl 5α-cholestane added prior to lipid extraction. Peak identifications were confirmed using GC/mass spectrometry (HP 6890 GC/MSD). The other part of the extract was filtered through a 0.45 μm, 4 mm diameter PTFE filter, and then analyzed for GDGTs, using an Agilent 1200 HPLC/6410 TripleQuad MS instrument equipped with an auto-injector and the Chemstation chromatography manager software, and according to the procedures described by Hopmans et al. (2000).

2.4. Dating

The ^{210}Pb method was used for dating; measurements were performed using ORTEC HPGe detectors (GEM, Lo-Ax and GMX) at the Institute of Earth Sciences, Academia Sinica, Taiwan (e.g., Huh et al., 2006). The international standard reference materials IAEA-133A, -327, and -375 were used to determine the energy, efficiency, and mass calibration of each detector. Constant ^{210}Pb activities in the lower portions of the cores were assumed to represent supported ^{210}Pb, and this value was subtracted from total activity to yield excess ^{210}Pb activity ($^{210}Pb_{ex}$). Sedimentation rates were calculated based on the decay (hence, decrease) of $^{210}Pb_{ex}$ with depth in the cores.

2.5. Degradation-corrected organic C concentration

The influence of diagenesis on downcore organic C concentration was evaluated using Middelburg's age-dependent model (Middelburg, 1989). This model is based on the assumption of a continuum of fractions with different degradabilities, and it appears to remain valid over eight orders of magnitude of time and rate constants ranging from laboratory fresh organic matter (e.g., recently collected plankton or algae), to field data from coastal, continental margin, and pelagic sediments (Middelburg, 1989). The model can predict the concentration of organic C at any time resulting from a constant input and steady state diagenesis process, according to the equation:

$$dC_t/dt = -k(t)C_t \quad (2)$$

where C_t is the concentration of organic C at time t, and k is the time-dependent kinetic constant for organic C degradation. k can be expressed as:

$$k = 0.16(a_0 + t)^{-0.95} \quad (3)$$

where a_0 is the apparent initial age that is determined by fitting the model to the downcore data (Middelburg, 1989):

$$C_t = C_0 \exp\left(3.2\left({a_0}^{0.05} - (a_0 + t)^{0.05}\right)\right) \quad (4)$$

where C_0 is the concentration of organic C at the sediment surface prior to sedimentary degradation loss, which we aim to calculate here. The magnitude of a_0 is a measure of the extent of organic matter alteration during settling through the overlying water column, whereby high values of a_0 indicate that a larger fraction of reactive compounds has been degraded during transit. The value of a_0 for each core site should be determined before C_0 for the sample being resolved.

To obtain a_0 for each core site, two C_t values were selected from its vertical asymptote to the organic C profile by assuming a steady state organic C burial flux; i.e., with the same C_0 values. This is plausible,

because the vertical asymptote of the organic C profile is in the lower section of the sediment cores, which were deposited when the impact of human activity was minimal. Then, a_0 for each site was determined by applying the two selected C_t values separately to Eq. (4). Finally, given a known a_0 value for a site, C_0 for any downcore sample deposited at time t was solved using Eq. (4).

We did not consider the degradation loss of biomarkers, because the time-dependent degradation constant for biomarkers is not well constrained. Instead, we used the organic C normalized biomarker concentration, which can greatly diminish the influence of diagenetic degradation on biomarker changes.

3. Results and discussion

3.1. Sediment chronology

Generally, each core shows a log-linear $^{210}Pb_{ex}$ profile when plotted against cumulative mass downcore (Fig. 2), thus the constant initial concentration (CIC) model was used for the calculation of mass accumulation rates (MARs) and the age of the sediments (Krishnaswami et al., 1971) (Table 1). Relatively uniform $^{210}Pb_{ex}$ activity was found in the near-surface layers of these cores, indicating a zone of bioturbation and sediment mixing (Nittrouer et al., 1979). These anomalies only have a significant effect on the chronology if the thickness of the disturbed zone exceeds about 15% of the depth of the $^{210}Pb_{ex}$ profile (Oldfield and Appleby, 1984). In our cores, as the thickness of the disturbed zone was within this limit, we assumed that mixing exerted a negligible effect. The specific cause of the jump in the lower part of $^{210}Pb_{ex}$ profile of core A6 is not clear at present, but it may be related to a break in deposition.

Spatially, MARs decrease from the inshore site (A9) to the distal site (A5), except at A7, where MAR is anomalously low (Table 1). The linear accumulation rate (LAR) at all sites was <1 cm year^{-1}. By contrast, the average modern sedimentation rate in the PRE is >1 cm year^{-1} (Owen, 2005). We tentatively attribute the low MAR at A7 to sediment winnowing associated with the seabed morphology or water circulation, and hence the historical sediment records, used to reconstruct past events, would have been compromised at this site. However, it is assumed here that the extent of sediment winnowing has remained constant over the time period represented by this core.

3.2. Terrestrial vs. marine sources of TOC

The study area has the potential to receive appreciable terrestrial organic matter (OM) inputs. In this study, we used two bulk parameters, the TOC:TN ratio and $\delta^{13}C_{org}$, and a recently introduced proxy, the branched and isoprenoid tetraether (BIT) index (Hopmans et al., 2004), to examine the terrestrial OC component of the sediment cores.

The average TOC content downcore decreased with distance offshore from 0.62% (range: 0.54% to 0.71%) at A9, to 0.51% (0.32% to 0.69%) at A7, 0.48% (0.33% to 0.72%) at A6, and 0.23% (0.16% to 0.39)

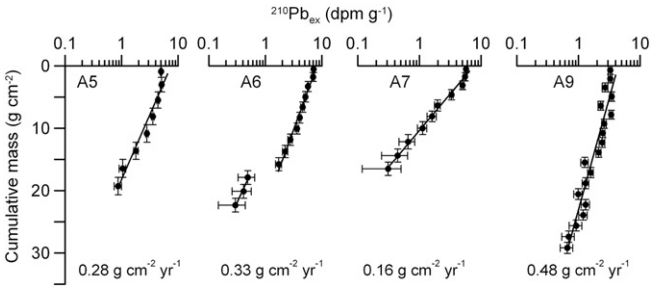

Fig. 2. Activity-cumulative mass profiles of $^{210}Pb_{ex}$ in the four sediment cores.

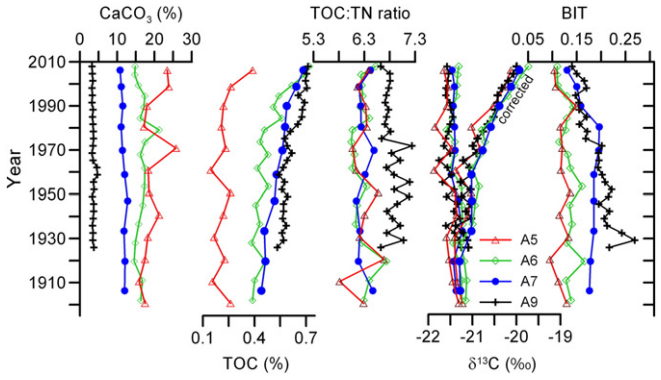

Fig. 3. Downcore variations in $CaCO_3$, TOC, the TOC:TN ratio, $\delta^{13}C_{org}$, fossil fuel-corrected $\delta^{13}C_{org}$, and BIT values.

at A5 (Fig. 3). This TOC distribution pattern is exactly opposite to that of $CaCO_3$ as the latter increases offshore from 3.6% (3.2% to 4.7%) at A9, to 11.7% (10.8% to 12.9%) at A7, 16.5% (14.6% to 21.3%) at A6, and 19.4% (15.9% to 25.8%) at A5. This $CaCO_3$ distribution may suggest increased production by marine calcifying organisms; e.g., coccolithophores, toward the open waters offshore. The TOC:TN ratio has a mean value of 6.8 (range: 6.6–7.2) inshore at A9, and a slightly lower mean value of 6.3 (5.8–6.7) in the three offshore cores, but showed no temporal trend and little variability (Fig. 3). TN probably occurs predominantly in the organic form, as indicated by its strong linear correlation ($r^2 > 0.95$) with TOC, and the negligible %TN intercept (between −0.008% and +0.003% for the four cores) at %TOC = 0 (Fig. 4). Values of $\delta^{13}C_{org}$ were similar in the four cores, being −21.51‰ ± 0.12‰ at A9, −21.40‰ ± 0.07‰ at A7, −21.36‰ ± 0.10‰ at A6, and −21.55‰ ± 0.18‰ at A5 (Fig. 3). The fossil fuel isotope-corrected $\delta^{13}C_{org\text{-}corr}$ values were also similar, ranging between −21.48‰ and −19.73‰. Both the TOC:TN ratio and $\delta^{13}C$ values recorded here fit with typical marine derived OM, and are distinct from terrestrially derived OM; the latter generally shows TOC:TN > 15, and $\delta^{13}C_{org} < -24\%$ for soils dominated by C_3 plants such as those that occur in the Pearl River catchments (Jia and Peng, 2003; Chen and Jia, 2009; Hu et al., 2009; Yu et al., 2010). These results are consistent with previous work in this region demonstrating that terrestrial OM contributes significantly to the PRE sediments, but much less so to the shelf sediments outside the PRE (Hu et al., 2009). Nevertheless, the slightly higher TOC:TN ratio and lighter $\delta^{13}C_{org}$ at the inshore site (A9) may suggest a minute, but perceptible, terrestrial OM influence.

The BIT index, a proxy for estimating the relative contribution of soil OM to marine sediments (Hopmans et al., 2004; Weijers et al.,

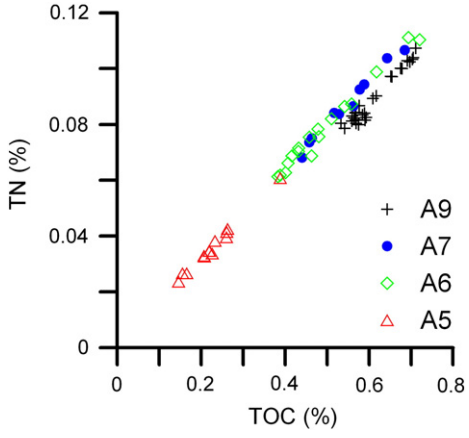

Fig. 4. Crossplot of total nitrogen vs. total organic carbon in the four sediment cores.

2006), decreases from >0.9 in the sediments at the freshwater entrance to around 0.2 at the mouth of the PRE (Strong et al., 2012), indicative of a decreasing soil OM contribution along the flow path from the terrestrial to the marine environment. This spatial distribution, together with those of TOC:TN and $\delta^{13}C_{org}$, demonstrates that the BIT index is a valid proxy for the relative contribution of terrestrial OM in the study area, and suggests that the PRE is an important trap for terrestrial OM. Downcore BIT index values in these four cores, which were typically <0.2 except in the lower section of A9 (Fig. 3), generally agree with TOC:TN and $\delta^{13}C_{org}$ profiles indicative of a predominant contribution of marine organic carbon (MOC). However, the more pronounced decrease in BIT values with distance offshore from A9 to A5 implies that BIT may be more sensitive to subtle changes in the terrestrial OM contribution, which is difficult to measure using the TOC:TN and $\delta^{13}C_{org}$ values. The accuracy of $\delta^{13}C_{org}$ and the TOC:TN ratio as source indicators could be reduced by several confounding factors, such as the wide range of end-member values and diagenetic alteration (Jia and Peng, 2003; Yu et al., 2010). For example, bulk soil $\delta^{13}C$ values can vary by >4‰ in the Pearl River catchments (Yu et al., 2010). Therefore, the use of BIT as an index for estimating MOC in sediments was preferred in this study.

The BIT index at the most distal site (A5) ranged from 0.09 to 0.15, whereas in terrestrial samples, including soils and river particulate matter, it varies from 0.90 to 0.99, with a mean of 0.95 (our unpublished data). The BIT index was first proposed to range from 0 (a completely marine origin) to 1 (a completely terrestrial origin). However, recent findings of terrestrial crenarchaeol indicate that the index is better interpreted as a range between 0 and 0.1 for marine-dominated samples, and between 0.8 and 1 for terrestrially dominated samples (Herfort et al., 2006; Walsh et al., 2008). In this study, BIT values of 0.05 and 0.95 were set for marine and terrestrial end members, respectively, to quantify the marine and terrestrial contributions to TOC. The results show that the contribution of terrestrial OC to TOC in the sediment cores is, on average, 16% ± 4% in A9, 14% ± 2% in A7, 9% ± 2% in A6, and 7% ± 2% in A5. The deceasing BIT value with time, together with the increasing TOC (Fig. 3), indicates that MOC accounts for progressively more of the sediment's TOC.

3.3. MOC record and inference for enhanced primary productivity

The downcore MOC content, calculated using the BIT index, has increased steadily since the early 20th century, except at the distal site (A5) where an MOC increase is not obvious until the turn of the 21st century (Fig. 5). This secular increase in MOC deposition could be caused by an increased MOC burial flux, time-dependent degradation of sediment OM, or enhanced OM preservation due, perhaps, to a decrease in the bottom water dissolved oxygen concentration. Here, enhanced OM preservation can be disregarded as a possible cause of the observed increase in MOC. According to Tyson (2001), when the LSR (linear sedimentation rate) is greater than 35 cm ka^{-1}, the preservation of autochthonous OM is largely independent of whether the bottom water is oxic or anoxic, and the MOC is a function only of OC input. Sedimentation rates at our study sites are 4–20 times above this threshold value.

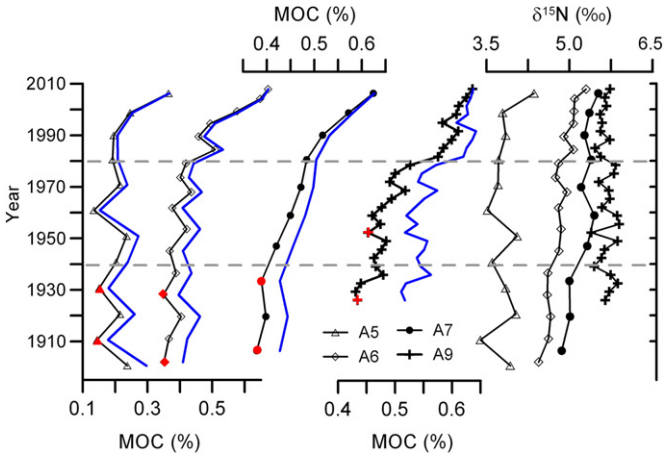

Fig. 5. Downcore profiles of MOC and $\delta^{15}N$. Blue curves are MOC_{corr}, and red symbols are selected MOC data points used for determination of a_0. See text for details. (For interpretation of the references to color in this figure, the reader is referred to the web version of this article.)

As explained above, we used the Middelburg's (1989) model to assess the influence of diagenesis and burial flux on the downcore changes to MOC. The selected MOC values for determination of a_0 at each site are shown as red symbols in Fig. 5, which yield a_0 values of 59, 128.5, 95, and 54.6 years, for sites A9, A7, A6, and A5, respectively. These apparent initial ages are well within the calculated range between values for the estuarine (<10 years) and oceanic (>100 years) sediments (Middelburg, 1989). The degradation loss after deposition accounts for 0.2% to 23.3% of the initial MOC (MOC_{corr}) at the sediment surface. Profiles of MOC_{corr} (blue curves in Fig. 5) follow those of MOC, indicating that the burial flux is responsible for the downcore changes in MOC at these sites. The MOC_{corr} profiles show that burial flux follows an asynchronous evolution, with the incipient increase beginning in the 1940s at sites A9 and A7, in the 1970s at A6, and after 2000 at the distal site A5. However, superimposed on this gradual and asynchronous trend, is a concurrent and more rapid increase in MOC burial flux since around 1980 at sites A9, A7, and A6.

The suggested MOC burial flux increases could be the result of enhanced primary productivity in the water column and/or increased MOC delivery efficiency. The former is supported by the coherence between the MOC_{corr} increases at sites A9, A7, and A6, and the $\delta^{13}C_{org\text{-}corr}$ records, with the latter showing a gradual increase of around 0.5‰ between 1940 and 1970, followed by a rapid increase of up to 1.0‰ after 1970 (Fig. 3). This temporal $\delta^{13}C_{org\text{-}corr}$ feature could be evidence of an increased MOC fraction in TOC due to enhanced primary productivity and/or higher phytoplankton growth rates in surface waters and the resultant carbon limitation (e.g., Hodell and Schelske, 1998; Zimmerman and Canuel, 2002; Turner et al., 2006). A recent report based on historical data also proposed that marine productivity in the study area has been increasing since at least the 1970s (Ning et al., 2009).

The downcore $\delta^{15}N$ records at sites A6 and A7, which exhibit progressive increases of around 0.6‰ from the 1940s to the 2000s (Fig. 5), could also support the enhanced primary productivity since the 1940s. In the coastal northern SCS, an increase of sedimentary $\delta^{15}N$ from around 4‰ offshore to >6‰ inshore, or in the PRE, has been previously documented (Hu et al., 2006; Zhang et al., 2009; Böttcher et al., 2010). This spatial pattern is clearly corroborated by our $\delta^{15}N$ records from offshore (3.8‰ ± 0.3‰ at A5) to inshore (5.7‰ ± 0.1‰ at A9) sites (Fig. 5). The influence of terrestrial OM in shaping such a spatial distribution can be discounted, because this would require higher $\delta^{15}N$ values for terrestrial OM, which is at odds with the relatively constant $\delta^{15}N$ at inshore site A9, and the increasing trend of $\delta^{15}N$ at sites A6 and A7. At these sites, BIT and $\delta^{13}C_{org\text{-}corr}$ records suggest that the contribution of terrestrial OM decreases with time (Fig. 3). Based on three lines of evidence, we argue that the higher $\delta^{15}N$ values recorded in this study reflect an increased terrestrial nutrient influx. Firstly, $\delta^{15}N$ of primary producers is thought to be a reliable indicator of the relative wastewater load to receiving waters and, to a lesser extent, of water-column dissolved inorganic N across a wide geographic carbon flow in marine and freshwater ecosystems (Cole et al., 2004). Meanwhile, sedimentary $\delta^{15}N$ records have been found to reflect eutrophication in the overlying water column (e.g., Zimmerman and Canuel, 2002; Turner et al., 2006). Secondly, the terrestrial nitrate end-member is ^{15}N-enriched in the Pearl River (between 1.9‰ and 17.6‰, averaging 7.9‰; Chen et al., 2009), and in coastal groundwater (between 6‰ and 26‰; Zhao et al.,

2008). Thirdly, $\delta^{15}N$ of the marine nitrate end-member, although not available currently, should be lower than its terrestrial counterpart because the particulate $\delta^{15}N$ in the upper 100 m of the open SCS was found to be 2.0‰ to 5.3‰, and such low values were attributed to marine N fixation (Kao et al., 2012). Therefore, the persistently higher $\delta^{15}N$ values (5.67‰ ± 0.14‰) inshore at site A9 may indicate that nutrient-derived ^{15}N has been influenced predominantly by terrestrial nutrients, and is thus insensitive to its influx over the time frame of these sediment cores. On the other hand, the progressive increases of $\delta^{15}N$ with time at offshore sites A6 and A7 toward the value at site A9, may suggest the enhanced influence of terrestrial nutrients. That $\delta^{15}N$ in the distal core (A5) remained low, except near the top of the core, is consistent with the MOC profile of the site, and suggests less impact from terrestrial nutrient influx until the turn of the century, when coastal pollution was aggravated by the increasingly rapid development in the Pearl River Delta.

The MOC and isotope records demonstrate that the increase in land-derived nutrient loadings has caused a rapid increase in primary production as far as site A6 on the shelf off the PRE since around 1980. This timing is consistent with the widely reported increases in the burial flux of bulk organic matter and algal markers (Hu et al., 2008; Hu et al., 2009), and anthropogenic trace elements and organic pollutants (Ip et al., 2004; Peng et al., 2007, 2008; Shi et al., 2010) in the PRE and nearby inshore area. These changes are closely associated with the rapid reclamation, urbanization, and industrialization of the Pearl River Delta region since the 1970s. As a result of enhanced anthropogenic activity, eutrophication, algal blooms, and red tides have frequently been reported in the northern coastal waters of the SCS (e.g., Liang et al., 2000; Yin, 2003).

Nevertheless, we note that the increase in $\delta^{15}N$ and $\delta^{13}C_{org\text{-}corr}$ in cores A6 and A7 began in 1940 and continued thereafter. Corresponding to these isotopic increases, is a slow increase of MOC_{corr} in core A7, and a nearly constant MOC_{corr} in core A6 (Fig. 5); the MOC_{corr} increase at A6 is not obvious until the 1980s. This discrepancy could be related to the greater distance of site A6 from the shore, which may lead to the delayed response of primary productivity to the increased human activity on land. However, the plankton community structure at A6 appears to respond to the fluvial nutrient load immediately, which may slow down the response of the marine carbon system, as will be discussed later. Here, it should be pointed out that the timing of the initial, gradual increase in MOC_{corr} around 1940 at sites A9 and A7, was also observed in other types of record extracted from the PRE and adjacent areas, including sedimentation rates (Owen and Lee, 2004), algal markers and coprostanol (a marker of domestic sewage) (Hu et al., 2008), and hydrocarbons (Liu et al., 2005; Peng et al., 2008). This is a period associated with wartime deforestation, and increasing urbanization, industrialization, and reclamation after World War II (Owen and Lee, 2004).

3.4. Changes in phytoplankton community structure

A variety of sterol distributions occur within the microalgae (Volkman et al., 1998). Although sterols are not highly species-specific markers, the similarity of their chemical structures helps to minimize the influence of diagenesis, and allows their ratios to be used to trace past changes in phytoplankton community structure (e.g., Schubert et al., 1998; Zimmerman and Canuel, 2002). Here, 24-methylcholesta-5,24(28)-dien-3β-ol ($28\Delta^{5,24(28)}$) and 4α,23,24-trimethyl-5α-cholest-22-en-3β-ol ($30\Delta^{22}$), the dominant sterols in diatoms and dinoflagellates, respectively, were selected as indicators for the two algae. In addition, 24-ethylcholest-5-en-3β-ol ($29\Delta^{5}$), a widespread sterol that occurs in 9 out of 14 microalga classes (Volkman et al., 1998), was selected to compare with $28\Delta^{5,24(28)}$ as an index for assessing the contribution of small-celled phytoplankton relative to diatoms, as assessed elsewhere (e.g., Zimmerman and Canuel, 2002). The sterol $29\Delta^{5}$ was considered to be a land plant biomarker in the PRE and northern SCS based on previous surface sediment studies (Hu et al., 2009; Strong et al., 2012). However, its downcore changes are similar to those of other phytoplankton biomarkers (Fig. 6), and opposite to the terrestrial contributions suggested by the BIT and $\delta^{13}C_{org\text{-}corr}$ records, indicating that downcore changes in $29\Delta^{5}$ were controlled mainly by algal input rather than terrestrial influx. All of these sterol compounds, except $28\Delta^{5,24(28)}$ in core A5, display similar patterns of upward enrichment relative to MOC; i.e., low concentrations in the early 20th century, a gradual increase during the mid-20th century, and a rapid increase after about 1980 (Fig. 6). This pattern is generally consistent with the MOC profiles described above, indicating, again, that enhanced primary productivity is the main cause of the MOC increase over the past three decades.

Biomarker ratios can be used to assess changes in the relative predominance of plankton groups. The ratios $30\Delta^{22}$:$28\Delta^{5,24(28)}$ and $29\Delta^{5}$:$28\Delta^{5,24(28)}$, suggestive of the relative abundance of dinoflagellates and non-diatom algae to diatoms, respectively, show an increasing trend since the 1940s at sites A7, A6, and A5 (Fig. 7). In contrast, no clear temporal trend can be seen in these two sterol ratios inshore at site A9, except a transient high during the period 1960–1975 (Fig. 7). It seems that diatom numbers decreased, while small-celled algae increased within the communities at sites A7, A6, and A5, whereas the community structure remained largely unchanged inshore at A9. Similarly to the sterol ratios, $\delta^{15}N$ also shows different depth profiles between the inshore and offshore sites, with progressive enrichment of ^{15}N since the 1940s at the two offshore sites (A7 and A6), and uniformly heavier values inshore at A9. This temporal and spatial correspondence between sterol ratios and $\delta^{15}N$ suggests that the shift in community structure at A7 and A6 may be attributable to terrestrial nutrient influx.

It has been observed recently that terrestrial nutrient influx can stimulate not only the growth of diatoms in the PRE and adjacent areas, but also the growth of picoplankton in the adjacent oligotrophic oceanic water (Qiu et al., 2010). During the summer monsoon period, a freshwater plume, which has high concentrations of nitrate but relatively low phosphate levels, can be observed at sites as far out as A6 (Dai et al., 2008b), indicating the export of excess N offshore into the northern SCS (Cai et al., 2004; Yin and Harrison, 2008; Qiu et al., 2010). This would cause P limitation to inhibit the growth of diatoms at the distal sites. Interestingly, picoplankton has indeed become an important primary producer in the offshore open waters over the past decade (Qiu et al., 2010). Inshore, at A9, the relatively stable community structure suggests that silica and/or phosphate limitations are not severe due to the proximity of the site to the mouth of the PRE. Therefore, diatoms are the dominant algae around this site (Huang et al., 2004; Dai et al., 2008b; Qiu et al., 2010).

Phytoplankton community structure is a key component of ecosystem functioning for carbon export. The greater abundance of diatoms, due to their larger sizes, is favorable to the downward sinking of carbon through either sedimentation of cells and phyto-detritus or in the feces of large metazoan grazers. In contrast, a phytoplankton

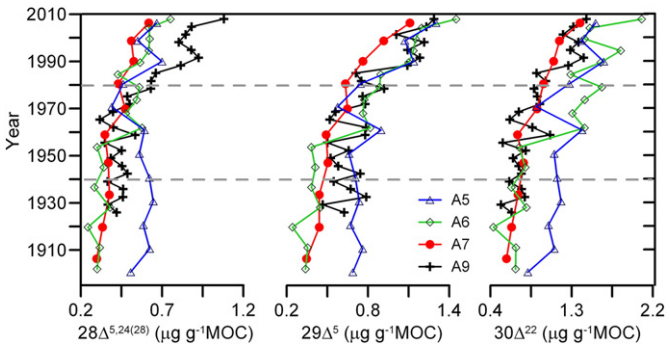

Fig. 6. Downcore profiles of MOC normalized sterol biomarker compound concentrations.

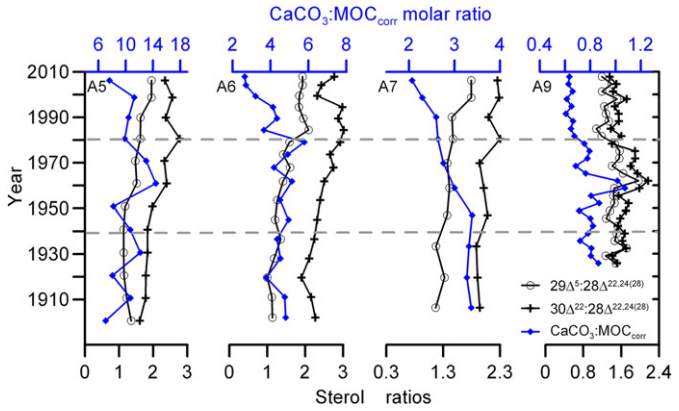

Fig. 7. Downcore profiles of $30\Delta^{22}$ (dinoflagellate sterol) and $29\Delta^{5}$ (non-diatom sterol) relative to $28\Delta^{5,24(28)}$ (diatom sterol), and of the molar ratio of $CaCO_3$ to MOC_{corr}.

community dominated by small-celled algae would result in the predominantly microbial recycling of OM, leading to high retention of carbon in the water column and, consequently, low downward carbon flux (Michaels and Silver, 1988; Boyd and Harrison, 1999; Jacquet et al., 2011). Therefore, the shifts in community structure since the 1940s suggested at sites A7 and A6 might have reduced the efficiency of carbon export, and therefore have offset the expected concurrent increase in primary productivity with nutrient influx indicated by the increase in $\delta^{15}N$. This is a likely scenario at site A6 during the period between 1940 and 1980, when there was a nearly constant MOC_{corr} level. It appears that the transient decreases in MOC_{corr} around 1960 and 1975 at A9 (Fig. 5) correspond to brief increases in small-celled algae (Fig. 7), also suggesting a decline in carbon export efficiency. After 1980, MOC_{corr} increased significantly at A7 and A6, and the main cause of this is likely to have been the growth of primary productivity as discussed above, but may also be related to the slowdown in the increase of non-diatom algae at these sites (Fig. 7). However, the gradual increase of MOC_{corr}, and relative decrease of diatoms in the community at site A7 between 1940 and 1980, suggest that changes in community structure may play a less significant role than primary productivity in controlling organic C export in this shallow coastal area.

Recent observations have shown that organic C export is closely correlated with fluxes of ballast minerals (calcium carbonate, opal, and lithogenic material), and that ballasting from carbonate is more efficient than from opal (Armstrong et al., 2002; Iversen and Ploug, 2010). Downcore change in the $CaCO_3$:MOC_{corr} molar ratio (Fig. 7) is therefore used here to infer changes in the calcifying organisms, mainly coccolithophores, and their contribution to MOC burial. Since 1980, the $CaCO_3$:MOC_{corr} ratio remained almost constant at A9, but decreased rapidly at A7 and A6. The decrease at A7 and A6 may suggest decreased carbonate production, and thus reduced organic C export via carbonate ballasting. This is the opposite of the significant increase in MOC_{corr} at the two sites since 1980. The decrease in the $CaCO_3$:MOC_{corr} ratio between 1940 and 1980 at site A7 is also opposite to the gradual increase of MOC_{corr}. Additionally, the relatively unchanged $CaCO_3$:MOC_{corr} ratio since 1980 at A9 is also in disagreement with the significant increase in MOC_{corr}. These observations suggest only a minor role for carbonate ballasting in organic C burial in our study area. This may be because the water depth is shallow and $CaCO_3$ productivity is low in this area relative to the bathypelagic zones of the ocean to which the hypothesis of ballast minerals for organic C export has been applied (Armstrong et al., 2002; Iversen and Ploug, 2010). In addition, the role of lithogenic ballast in modulating organic C export is unlikely to be important either, because we assumed earlier that MAR, being predominantly determined by terrestrial materials, is constant based on the ^{210}Pb profiles.

At the distal site A5, there is no change in $\delta^{15}N$ that corresponds to the shift in sterol-inferred phytoplankton community structure. In addition, $28\Delta^{5,24(28)}$ inferred diatoms, which are more sensitive to eutrophication and the freshwater plume (e.g., Dai et al., 2008b), does not increase with time. The $CaCO_3$:MOC_{corr} ratio also shows no secular trend. This implies that terrestrial nutrient influx is unlikely to be the cause of the community shift. An earlier investigation showed that the summer freshwater plume and associated phytoplankton bloom did not reach this distal site (Dai et al., 2008b). It is probable then that other environmental factors, such as seawater temperature, salinity, and circulation, were responsible for the changes in community structure at this site, and these factors should also be considered with respect to the changes at the other three sites in a future study.

4. Implications for coastal marine carbon metabolism

Marine organic metabolism (i.e., the difference between primary production by photosynthesis and organic oxidation by respiration) in the coastal ocean has attracted increasing attention over recent decades due to its potential role in the oceanic carbon budget and its vulnerability to human activities and climate change (Smith and Hollibaugh, 1993; Cai et al., 2003; Borges et al., 2005; Chen and Borges, 2009; Cai, 2011). In the PRE, a shift from net respiration in the upper reaches (aqueous pCO_2 up to several thousands μatm), to net community production in the lower reaches (pCO_2 below or near the atmospheric level), has been observed (Zhai et al., 2005; Chen et al., 2008b; Guo et al., 2008). The organic metabolism on the shelf area outside the PRE remains elusive, although a heterotrophic state, and hence potentially a source of atmospheric CO_2, was proposed by Chen et al. (2008). However, a freshwater plume emptying into the shelf appears to stimulate primary production and to act as a sink for CO_2 (Guo et al., 2008; Chen et al., 2012). Our MOC_{corr} records from cores A9, A7, and A6, characterized by rapid increases since about 1980, are most probably related to the influx of fluvial nutrients. They indicate the non-steady state of the marine ecosystem over the past 30 years, in which organic matter produced from inorganic nutrients has been increasingly exported out of the production–respiration cycle. Although this situation cannot be viewed as evidence of net production, it may suggest that the scale of organic metabolism at these sites has probably been tipping in favor of autotrophy. A number of modeling studies have explored the impact of increased nutrient and carbon loads on the organic metabolism and direction of air–sea CO_2 exchange in coastal areas and seem to support this scenario, as they show that coastal waters have recently switched, or will soon switch, from being a net source to a net sink of CO_2, because of rising atmospheric CO_2 levels and eutrophication (Ver et al., 1999; Rabouille et al., 2001; Andersson and Mackenzie, 2004; Mackenzie et al., 2004; Gypens et al., 2009). Therefore, eutrophication in the coastal northern SCS appears to have contributed, or will contribute, to the sequestration of atmospheric CO_2. However, the relative decrease in diatoms, and increase in small-celled algae, recorded here within the community structure at offshore sites A7 and A6 require further consideration, because pico- and nanoplankton usually contribute less to vertical export and are more involved in regenerative cycling (Carlson et al., 1998; Boyd and Harrison, 1999; Jacquet et al., 2011), which would partially offset the effect of the expected increase in primary production (e.g., Gypens et al., 2009; Jacquet et al., 2011).

However, while organic matter production provides a sink for atmospheric CO_2, carbonate formation via marine calcifying organisms causes an increase in surface water pCO_2 and therefore acts as a potential source of CO_2 to the atmosphere (Frankignoulle et al., 1994; Zondervan et al., 2001). In this study, the decrease in the $CaCO_3$:MOC_{corr} ratio over the past 30 years at A9, A7, and A6, suggesting a relative slowdown of $CaCO_3$ production in the surface water, may have created a negative feedback limiting the rise in atmospheric CO_2 (Riebesell et al., 2000; Barker et al., 2003). Consequently, this

factor should also be taken into account when attempting to predict the role of the coastal northern SCS in mitigating future anthropogenic CO_2 increases.

Acknowledgments

We thank the expedition chief scientists, P. Cai and W. Zhai, and the crew of the *Dongfanghong II* for their support and help during the cruises. The cruise and laboratory studies were supported by the National Basic Research Program of China (2009CB421206), the National Natural Science Foundation of China (no. 41061160498), and the NSC through grant NSC97-2611-M-001-002-MY3. We are grateful to two anonymous reviewers for their valuable comments, which helped to improve this paper. This is contribution No. IS-1634 from GIGCAS.

References

Andersson, A.J., Mackenzie, F.T., 2004. Shallow-water oceans: a source or sink of atmospheric CO_2? Front. Ecol. Environ. 2, 348–353.
Armstrong, R.A., Lee, C., Hedges, J.I., Honjo, S., Wakeham, S.G., 2002. A new, mechanistic model for organic carbon fluxes in the ocean based on the quantitative association of POC with ballast minerals. Deep-Sea Res. II 49, 219–236.
Barker, S., Higgins, J.A., Elderfield, H., 2003. The future of the carbon cycle: review, calcification response, ballast and feedback on atmospheric CO_2. Philos. Trans. R. Soc. Lond. A 361, 1977–1999.
Borges, A.V., Delille, B., Frankignoulle, M., 2005. Budgeting sinks and sources of CO_2 in the coastal ocean: diversity of ecosystems counts. Geophys. Res. Lett. 32, L14601. http://dx.doi.org/10.1029/2005GL023053.
Böttcher, M.E., Voss, M., Schulz-Bull, D., Schneider, R., Leipe, T., Knöller, K., 2010. Environmental changes in the Pearl River estuary (China) as reflected by light stable isotopes and organic contaminants. J. Mar. Syst. 82, S43–S53.
Boyd, P., Harrison, P.J., 1999. Phytoplankton dynamics in the NE subarctic Pacific. Deep-Sea Res. II 46, 2405–2432.
Broecker, W.S., Peng, T.-H., 1974. Gas exchange rates between air and sea. Tellus 26, 21–35.
Cai, W.-J., 2011. Estuarine and coastal ocean carbon paradox: CO_2 sinks or sites of terrestrial carbon incineration? Annu. Rev. Mar. Sci. 3, 123–145.
Cai, W.-J., Wang, Z.A., Wang, Y., 2003. The role of marsh-dominated heterotrophic continental margins in transport of CO_2 between the atmosphere, the land–sea interface and the ocean. Geophys. Res. Lett. 30, 1849. http://dx.doi.org/10.1029/2003GL017633.
Cai, W.-J., Dai, M.H., Wang, Y.C., Zhai, W.D., Huang, T., Chen, S.T., Zhang, F., Chen, Z.Z., Wang, Z.H., 2004. The biogeochemistry of inorganic carbon and nutrients in the Pearl River estuary and the adjacent Northern South China Sea. Cont. Shelf Res. 24, 1301–1319.
Carlson, C.A., Ducklow, H.W., Hansell, D.A., Smith, W.O., 1998. Organic carbon partitioning during spring phytoplankton blooms in the Ross Sea polynya and the Sargasso Sea. Limnol. Oceanogr. 43, 375–386.
Chen, C.-T.A., Borges, A.V., 2009. Reconciling opposing views on carbon cycling in the coastal ocean: continental shelves as sinks and near-shore ecosystems as sources of atmospheric CO_2. Deep-Sea Res. II 56, 578–590.
Chen, F.J., Jia, G.D., 2009. Spatial and seasonal variations in $\delta^{13}C$ and $\delta^{15}N$ of particulate organic matter in a dam-controlled subtropical river. River Res. Appl. 25, 1169–1176.
Chen, C.-T.A., Wang, S.-L., Lu, X.-X., Zhang, S.-R., Lui, H.-K., Tseng, H.-C., Wang, B.-J., Huang, H.-I., 2008. Hydrogeochemistry and greenhouse gases of the Pearl River, its estuary and beyond. Quat. Int. 186, 79–90.
Chen, F.J., Jia, G.D., Chen, J.Y., 2009. Nitrate sources and watershed denitrification inferred from nitrate dual isotopes in the Beijiang River, south China. Biogeochemistry 94, 163–174.
Chen, C.-T.A., Huang, T.-H., Fu, Y.-H., Bai, Y., He, X., 2012. Strong sources of CO_2 in upper estuaries become sinks of CO_2 inlarge river plumes. Curr. Opin. Environ. Sustainability 4, 179–185.
Cloern, J.E., 2001. Our evolving conceptual model of the coastal eutrophication problem. Mar. Ecol. Prog. Ser. 210, 223–253.
Cole, M.L., Valiela, I., Kroeger, K.D., Tomasky, G.L., Cebrian, J., Wigand, C., McKinney, R.A., Grady, S.P., Carvalho da Silva, M.H., 2004. Assessment of a $\delta^{15}N$ isotopic method to indicate anthropogenic eutrophication in aquatic ecosystems. J. Environ. Qual. 33, 124–132.
Dai, M.H., Guo, X.H., Zhai, W.D., Yuan, L.Y., Wang, B.W., Wang, L.F., Cai, P.H., Tang, T.T., Cai, W.-J., 2006. Oxygen depletion in the upper reach of the Pearl River estuary during a winter drought. Mar. Chem. 102, 159–169.
Dai, M.H., Wang, L., Guo, X.H., Zhai, W.D., Li, Q., He, B., Kao, S.-J., 2008a. Nitrification and inorganic nitrogen distribution in a large perturbed river/estuarine system: the Pearl River Estuary, China. Biogeosci. 5, 1227–1244.
Dai, M.H., Zhai, W.D., Cai, W.-J., Callahan, J., Huang, B.Q., Shang, S.L., Huang, T., Li, X.L., Lu, Z.M., Chen, W.F., Chen, Z.Z., 2008b. Effects of an estuarine plume-associated bloom on the carbonate system in the lower reaches of the Pearl River estuary and the coastal zone of the northern South China Sea. Cont. Shelf Res. 28, 1416–1423.
Diaz, R.J., Rosenberg, R., 2008. Spreading dead zones and consequences for marine ecosystems. Science 321, 926–929.
Dong, L.X., Su, J.L., Wong, L.A., Cao, Z.Y., Chen, J.-C., 2004. Seasonal variation and dynamics of the Pearl River plume. Cont. Shelf Res. 24, 1761–1777.
Frankignoulle, M., Canon, C., Gattuso, J.-P., 1994. Marine calcification as a source of carbon dioxide: positive feedback of increasing atmospheric CO_2. Limnol. Oceanogr. 39, 458–462.
Gattuso, J.P., Frankignoulle, M., Wollast, R., 1998. Carbon and carbonate metabolism in coastal aquatic ecosystems. Annu. Rev. Ecol. Evol. Syst. 29, 405–434.
Guo, X.H., Dai, M.H., Zhai, W.D., Cai, W.-J., Chen, B.S., 2008. CO_2 flux and seasonal variability in a large subtropical estuarine system, the Pearl River estuary, China. J. Geophys. Res. 114, G03013. http://dx.doi.org/10.1029/2008JG000905.
Gypens, N., Borges, A.V., Lancelot, C., 2009. Effect of eutrophication on air–sea CO_2 fluxes in the coastal Southern North Sea: a model study of the past 50 years. Global Chang. Biol. 15, 1040–1056.
Herfort, L., Schouten, S., Boon, J.P., Woltering, M., Baas, M., Weiers, J.W.H., Sinninghe Damsté, J.S., 2006. Characterization of transport deposition of terrestrial organic matter in the southern North Sea using the BIT index. Limnol. Oceanogr. 51, 2196–2205.
Hodell, D.A., Schelske, C.L., 1998. Production, sedimentation, and isotopic composition of organic matter in Lake Ontario. Limnol. Oceanogr. 43, 200–214.
Hopmans, E.C., Schouten, S., Pancost, R.D., Van der Meer, M.T.J., Sinninghe Damsté, J.S., 2000. Analysis of intact tetraether lipids in archaeal cell material and sediments by high performance liquid chromatography/atmospheric pressure chemical ionization mass spectrometry. Rapid Commun. Mass Spectrom. 14, 585–589.
Hopmans, E.C., Weijers, J.W.H., Schefuß, E., Herfort, L., Sinninghe Damsté, J.S., Schouten, S., 2004. A novel proxy for terrestrial organic matter in sediments based on branched and isoprenoid tetraether lipids. Earth Planet. Sci. Lett. 224, 107–116.
Hu, J.F., Peng, P.A., Jia, G.D., Mai, B.X., Zhang, G., 2006. Distribution and sources of organic carbon, nitrogen and their isotopes in sediments of the subtropical Pearl River estuary and adjacent shelf, Southern China. Mar. Chem. 98, 274–285.
Hu, J.F., Zhang, G., Li, K.C., Peng, P.A., Chivas, A.R., 2008. Increased eutrophication offshore Hong Kong, China, during the past 75 years; evidence from high-resolution sedimentary records. Mar. Chem. 110, 7–17.
Hu, J.F., Sun, X.S., Peng, P.A., Zhang, G., Chivas, A.R., 2009. Spatial and temporal variation of organic carbon in the northern South China Sea revealed by sedimentary records. Quat. Int. 206, 46–51.
Huang, X., Huang, L., Yue, W., 2003. The characteristics of nutrients and eutrophication in the Pearl River estuary, South China. Mar. Pollut. Bull. 47, 30–36.
Huang, L.M., Jian, W.J., Song, X.Y., Huang, X.P., Liu, S., Qian, P.Y., Yin, K.D., Wu, M., 2004. Species diversity and distribution for phytoplankton of the Pearl River estuary during rainy and dry seasons. Mar. Pollut. Bull. 49, 588–596.
Huh, C.-A., Su, C.-C., Wang, C.-H., Lee, S.-Y., Lin, I.-T., 2006. Sedimentation in the southern Okinawa Trough — rates, turbidites and a sediment budget. Mar. Geol. 231, 129–139.
Ip, C.C.M., Li, X.D., Zhang, G., Farmer, J.G., Wai, O.W.H., Li, Y.S., 2004. Over one hundred years of trace metal fluxes in the sediments of the Pearl River estuary, South China. Environ. Pollut. 132, 157–172.
Iversen, M.H., Ploug, H., 2010. Ballast minerals and the sinking carbon flux in the ocean: carbon-specific respiration rates and sinking velocity of marine snow aggregates. Biogeosci. 7, 2613–2624.
Jacquet, S.H.M., Lam, P.J., Trull, T., Dehairs, F., 2011. Carbon export production in the subantarctic zone and polar front zone south of Tasmania. Deep-Sea Res. II 58, 2277–2292.
Jia, G.D., Peng, P.A., 2003. Temporal and spatial variations in signatures of sedimented organic matter in Lingding Bay (Pearl estuary), southern China. Mar. Chem. 82, 47–54.
Kao, S.J., Yang, J.Y.T., Liu, K.K., Dai, M.H., Chou, W.-C., Lin, H.L., Ren, H.J., 2012. Isotope constraints on particulate nitrogen source and dynamics in the upper water column of the oligotrophic South China Sea. Global Biogeochem. Cycles 26, GB2033. http://dx.doi.org/10.1029/2011GB004091.
Kemp, W.M., Smith, E.M., Marvin-DiPasquale, M., Boynton, W.R., 1997. Organic carbon-balance and net ecosystem metabolism in Chesapeake Bay. Mar. Ecol. Prog. Ser. 150, 229–248.
Krishnaswami, S., Lal, D., Martin, J.M., Meybeck, M., 1971. Geochronology of lake sediments. Earth Planet. Sci. Lett. 11, 407–414.
Liang, S., Qian, H.L., Qi, Y.Z., 2000. Problem on the red ride in coastal China Sea. Ecol. Sci. 19, 44–50 (in Chinese).
Liu, G.Q., Zhang, G., Li, X.D., Li, J., Peng, X.Z., Qi, S.H., 2005. Sedimentary record of polycyclic aromatic hydrocarbons in a sediment core from the Pearl River estuary, South China. Mar. Pollut. Bull. 51, 912–921.
Liu, Q., Dai, M., Chen, W., Huh, C.A., Wang, G., Li, Q., Charette, M.A., 2012. How significant is submarine groundwater discharge and its associated dissolved inorganic carbon in a river-dominated shelf system? Biogeosci. 9, 1777–1795.
Lynch-Stieglitz, J., Stocker, T.F., Broecker, W.S., Fairbanks, R.G., 1995. The influence of air–sea exchange on the isotopic composition of oceanic carbon: observations and modelling. Global Biogeochem. Cycles 9, 653–665.
Mackenzie, F.T., Lerman, A., Andersson, A.J., 2004. Past and present of sediment and carbon biogeochemical cycling models. Biogeosci. 1, 11–32.
Michaels, A.F., Silver, M.W., 1988. Primary production, sinking fluxes and the microbial food web. Deep-Sea Res. A 35, 473–490.
Middelburg, J.J., 1989. A simple model for organic matter decomposition in marine sediments. Geochim. Cosmochim. Acta 53, 1577–1581.
Ning, X., Lin, C., Hao, Q., Liu, C., Le, F., Shi, J., 2009. Long term changes in the ecosystem in the northern South China Sea during 1976–2004. Biogeosci. 6, 2227–2243.
Nittrouer, C.A., Sternberg, R.W., Caepenter, R., Bennett, J.T., 1979. The use of Pb-210 geochronology as a sedimentological tool: application to the Washington continental shelf. Mar. Geol. 31, 297–316.
Oldfield, F., Appleby, P.G., 1984. A combined radiometric and mineral magnetic approach to recent geochronology in lakes affected by catchments disturbance and sediment redistribution. Chem. Geol. 44, 67–83.
Owen, R.B., 2004. Modem fine-grained sedimentation — spatial variability and environmental controls on an inner pericontinental shelf, Hong Kong. Mar. Geol. 214, 1–26.

Owen, R.B., Lee, R., 2004. Human impacts on organic matter sedimentation in a proximal shelf setting, Hong Kong. Cont. Shelf Res. 24, 583–602.
Peng, X.Z., Wang, Z.D., Mai, B.X., Chen, F.R., Chen, S.J., Tan, J.H., Yu, Y.Y., Tang, C.M., Li, K.C., Zhang, G., Yang, C., 2007. Temporal trends of nonylphenol and bisphenol A contamination in the Pearl River estuary and the adjacent South China Sea recorded by dated sedimentary cores. Sci. Total. Environ. 384, 393–400.
Peng, X.Z., Wang, Z.D., Yu, Y.Y., Tang, C.M., Lu, H., Xu, S.P., Chen, F.R., Mai, B.X., Chen, S.J., Li, K.C., Yang, C., 2008. Temporal trends of hydrocarbons in sediment cores from the Pearl River estuary and the northern South China Sea. Environ. Pollut. 156, 442–448.
Qiu, D.J., Huang, L.M., Zhang, J.L., Lin, S.J., 2010. Phytoplankton dynamics in and near the highly eutrophic Pearl River estuary, South China Sea. Cont. Shelf Res. 30, 177–186.
Rabouille, C., Mackenzie, F.T., Ver, L.M., 2001. Influence of the human perturbation on carbon, nitrogen, and oxygen biogeochemical cycles in the global coastal ocean. Geochim. Cosmochim. Acta 65, 3615–3639.
Riebesell, U., Zondervan, I., Rost, B., Tortell, P.D., Zeebe, R.E., Morel, F.M.M., 2000. Reduced calcification of marine plankton in response to increased atmospheric CO_2. Nature 407, 364–367.
Schelske, C.L., Hodell, D.A., 1995. Using carbon isotopes of bulk sedimentary organic matter to reconstruct the history of nutrient loading and eutrophication in Lake Erie. Limnol. Oceanogr. 40, 918–929.
Schubert, C.J., Villanueva, J., Calvert, S.E., Cowie, G.L., von Rad, U., Schulz, H., Berner, U., Erlenkeuser, H., 1998. Stable phytoplankton community structure in the Arabian Sea over the past 200,000 years. Nature 394, 563–566.
Shi, J.-B., Ip, C.C.M., Zhang, G., Jiang, G.-B., Li, X.-D., 2010. Mercury profiles in sediments of the Pearl River estuary and the surrounding coastal area of South China. Environ. Pollut. 158, 1974–1979.
Smith, S.V., Hollibaugh, J.T., 1993. Coastal metabolism and the oceanic carbon balance. Rev. Geophys. 31, 75–89.
Smith, S.V., Swaney, D.P., Talaue-Mcmanus, L., Bartley, J.D., Sandhei, P.T., McLaughlin, C.J., Dupra, V.C., Crossland, C.J., Buddemeier, R.W., Maxwell, B.A., Wulff, F., 2003. Humans, hydrology, and the distribution of inorganic nutrient loading to the ocean. Bioscience 53, 235–245.
Strong, D.J., Flecker, R., Valdes, P., Wilkinson, I.P., Rees, J.G., Zong, Y.Q., Lloyd, J.M., Garrett, E., Pancost, R.D., 2012. Organic matter distribution in the modern sediments of the Pearl River estuary. Org. Geochem. 49, 68–82.
Su, J.L., 2004. Overview of the South China Sea circulation and its influence on the coastal physical oceanography outside the Pearl River estuary. Cont. Shelf Res. 24, 1745–1760.
Thomas, H., Bozec, Y., Elkalay, K., de Baar, H.J.W., 2004. Enhanced open ocean storage of CO_2 from shelf sea pumping. Science 304, 1005–1008.
Turner, R.E., Rabalais, N.N., Fry, B., Atilla, N., Milan, C.S., Lee, J.M., Normandeau, C., Oswald, T.A., Swenson, E.M., Tomasko, D.A., 2006. Paleo-indicators and water quality change in the Charlotte Harbor Estuary (Florida). Limnol. Oceanogr. 51, 518–533.
Tyson, R.V., 2001. Sedimentation rate, dilution, preservation and total organic carbon: some results of a modeling study. Org. Geochem. 32, 333–339.
Van Beusekom, J.E.E., de Jonge, V.N.N., 2002. Long-term changes in Wadden-Sea nutrient cycles: importance of organic matter import from the North Sea. Hydrobiology 475/476, 185–194.
Ver, L.M., Mackenzie, F.T., Lerman, A., 1999. Carbon cycle in the coastal zone: effects of global perturbations and changes in the past three centuries. Chem. Geol. 159, 283–304.
Volkman, J.K., Barrett, S.M., Blackburn, S.I., Mansour, M.P., Sikes, E.L., Gelin, F., 1998. Microalgal biomarkers: a review of recent research developments. Org. Geochem. 29, 1163–1179.
Walsh, E.M., Ingalls, A.E., Keil, R.G., 2008. Sources transport of terrestrial organic matter in Vancouver Island fjords the Vancouver–Washington Margin. A multiproxy approach using $\delta^{13}C$(org), lignin phenols, and the ether lipid BIT index. Limnol. Oceanogr. 53, 1054–1063.
Weijers, J.W.H., Schouten, S., Spaargaren, O.C., Sinninghe Damsté, J.S., 2006. Occurrence and distribution of tetraether membrane lipids in soils: implications for the use of the TEX86 proxy and the BIT index. Org. Geochem. 37, 1680–1693.
Yin, K.D., 2003. Influence of monsoons and oceanographic processes on red tides in Hong Kong waters. Mar. Ecol. Prog. Ser. 262, 27–41.
Yin, K.D., Harrison, P.J., 2008. Nitrogen over enrichment in subtropical Pearl River estuarine coastal waters: possible causes and consequences. Cont. Shelf Res. 28, 1435–1442.
Yin, K.D., Qian, P.Y., Chen, J.C., Hsieh, D.P.H., Harrison, P.J., 2000. Dynamics of nutrients and phytoplankton biomass in the Pearl River estuary and adjacent waters of Hong Kong during summer: preliminary evidence for phosphorus and silicon limitation. Mar. Ecol. Prog. Ser. 194, 295–305.
Yin, K.D., Qian, P.Y., Wu, M.C.S., Chen, J.C., Huang, L.M., Song, X.Y., Jian, W.J., 2001. Shift from P to N limitation of phytoplankton biomass across the Pearl River estuarine Plume during summer. Mar. Ecol. Prog. Ser. 221, 17–28.
Yin, K.D., Zhang, J.L., Qian, P.-Y., Jian, W.J., Huang, L.M., Chen, J.F., Wu, M.C.S., 2004. Effect of wind events on phytoplankton blooms in the Pearl River estuary during summer. Cont. Shelf Res. 24, 1909–1923.
Yu, F.L., Zong, Y.Q., Lloyd, J.M., Huang, G.Q., Leng, M.J., Kendrick, C., Lamb, A.L., Yim, W.W.S., 2010. Bulk organic $\delta^{13}C$ and C/N as indicators for sediment sources in the Pearl River delta estuary, southern China. Estuar. Coast. Shelf Sci. 87, 618–630.
Zhai, W.D., Dai, M.H., Cai, W.-J., Wang, Y.C., Wang, Z.H., 2005. High partial pressure of CO_2 and its maintaining mechanism in a subtropical estuary: the Pearl River estuary, China. Mar. Chem. 93, 21–32.
Zhang, L., Yin, K.D., Wang, L., Chen, F.R., Zhang, D.R., Yang, Y.Q., 2009. The sources and accumulation rate of sedimentary organic matter in the Pearl River estuary and adjacent coastal area, Southern China. Estuar. Coast. Shelf Sci. 85, 190–196.
Zhao, X.F., Chen, F.J., Chen, J.Y., Tang, C.Y., Luo, Y.L., Jia, G.D., 2008. Using nitrogen isotope to identify the sources of nitrate contamination in urban groundwater — a case study in Zhuhai City. Hydrogeol. Eng. Geol. 3, 87–92 (In Chinese).
Zimmerman, A.R., Canuel, E.A., 2002. Sediment geochemical records of eutrophication in the mesohaline Chesapeake Bay. Limnol. Oceanogr. 47, 1084–1093.
Zondervan, I., Zeebe, R.E., Rost, B., Riebesell, U., 2001. Decreasing marine biogenic calcification: a negative feedback on rising atmospheric pCO_2. Global Biogeochem. Cycles 15, 507–516.